Molecular Crystals and Liquid Crystals Science and Technology. Section A. Molecular Crystals and Liquid Crystals

Publication details, including instructions for authors and subscription information:
http://www.tandfonline.com/loi/gmcl19

A Calorimetric Determination of Fundamental Properties of Polymer-Dispersed Liquid Crystals

George W. Smith [a] , George M. Ventouris [b] & John L. West [b]

[a] Physics Department, General Motors Research Laboratories, Warren, Michigan, 48090-9055

[b] Liquid Crystal Institute, Kent State University, Kent, OH, 44242-0001

Version of record first published: 24 Sep 2006.

To cite this article: George W. Smith , George M. Ventouris & John L. West (1992): A Calorimetric Determination of Fundamental Properties of Polymer-Dispersed Liquid Crystals, Molecular Crystals and Liquid Crystals Science and Technology. Section A. Molecular Crystals and Liquid Crystals, 213:1, 11-30

To link to this article: http://dx.doi.org/10.1080/10587259208028713

Mol. Cryst. Liq. Cryst., 1992, Vol. 213, pp. 11–30
Reprints available directly from the publisher
Photocopying permitted by license only

Printed in the United States of America

A Calorimetric Determination of Fundamental Properties of Polymer-Dispersed Liquid Crystals

GEORGE W. SMITH

Physics Department, General Motors Research Laboratories, Warren, Michigan 48090-9055

and

GEORGE M. VENTOURIS and JOHN L. WEST

Liquid Crystal Institute, Kent State University, Kent, OH 44242-0001

(Received June 1, 1991; in final form August 9, 1991)

We have developed a combined calorimetric/electron microscopic technique for determining several fundamental properties of polymer-dispersed liquid crystal (PDLC) films. Calorimetry allows us to determine the solubility limit of liquid crystal in the polymer matrix as well as the fraction of liquid crystal which is dispersed in the form of microdroplets. By combining the calorimetry results with electron microscopy measurements of D, the microdroplet diameter, we are able to calculate the functional relationship between the droplet number density and D. All of these parameters are of considerable importance in assessing the behavior of PDLCs. The usefulness of the method is illustrated by applying it to thermally-cured epoxy-based systems.

Keywords: polymer-dispersed liquid crystals; liquid crystals; phase behavior; calorimetry; PDLC properties

INTRODUCTION

Polymer-dispersed liquid crystal (PDLC) films, dispersions of micron-sized droplets of liquid crystal (LC) in a polymer matrix, have considerable potential for a variety of applications, including information displays and privacy windows. It has been shown[1–3] that the electro-optic properties of PDLC films depend strongly on D, the diameter, and n_V, the volumetric number density, of the LC droplets. In forming a film, one seeks to optimize the electro-optic properties by proper choice of D and n_V.

At the same time it is, of course, desirable to minimize the amount of liquid crystal used in film fabrication. Thus, it is important to maximize the amount of LC entrapped in the microdroplets and minimize that dissolved in the polymer matrix. Therefore, one wishes to use a LC/polymer matrix combination for which A, the liquid crystal solubility limit in the matrix, is low. A low value of A enhances the degree of phase separation of LC from the cured matrix and thus helps to maximize α, the fraction of liquid crystal in the droplets. From this discussion, it is obviously important to be able to determine accurate values of A, α, D, and n_V.

It is our purpose to describe calorimetric methods which allow us to determine A and α and, in conjunction with electron microscopy measurements of D, to calculate n_V.

In the next three sections, we shall i) describe our experimental techniques, ii) present results of our studies of three epoxy-based PDLC systems, and iii) discuss the implications of these studies.

EXPERIMENTAL ASPECTS

Materials and Sample Preparation

The three PDLCs were of two main types: i) two systems each composed of a single component liquid crystal (5CB or 7CB) and a two-part epoxy, and ii) one system utilizing a multicomponent LC (E7) and an index-matched epoxy. For system i) samples having several LC concentrations were polymerized at a single cure temperature (T_{cure} = 40°C). Type ii) samples we prepared at three cure temperatures, again using several compositions. Details of sample preparation are described in the following paragraphs.

Type i. The epoxy, a two part system composed of a resin (Salda Rapido A) and a curing agent (Salda Rapido B) was obtained from Bostik.[4] The liquid crystals were 4-*n*-pentyl-4′-cyanobiphenyl (5CB) and 4-*n*-heptyl-4′-cyanobiphenyl (7CB).[5] The 5CB/Bostik PDLC was of especial interest because it had been studied previously by Golemme *et al.*[6] They showed that the nematic-isotropic transition changes from first order to continuous as droplet diameter decreases below 0.035 μm for LC concentrations less than about 20 weight percent.

Our type i) samples were prepared in an identical manner to that of Reference 6. Salda Repido parts A and B were mixed in a 1:1 ratio; various amounts of liquid crystals were added to give 12 samples (6 with 5CB, 6 with 7CB) having LC concentrations, X, of 17, 19, 21, 33, 38, and 42 weight percent. In addition, a sample containing no liquid crystal was prepared. After mixing, the samples were thoroughly stirred, centrifuged to eliminate air bubbles, poured into plastic containers, and then placed in an oven at 40°C for four hours, resulting in fully-cured cylindrical sample slugs about 5 mm in diameter. Since our preparation technique and compositions were the same as those of Reference 6, we used their droplet diameter measurements in analyzing our 5CB/Bostik results.

Type ii. In this case the epoxy was a three part system, containing the following weight percentages of components: 15.2% Epon resin 828,[7] 28.5% WC-97 resin,[8] and 56.3% Capcure 3-800 curing agent.[7] This choice of epoxy composition produced a matrix having a refractive index well matched to the ordinary index of the liquid crystal. The liquid crystal E7, a four-component mixture of substituted biphenyls and a terphenyl, was obtained from EM Chemicals.[5] Three sets of samples, each having E7 compositions of 0, 25, 30, 35, 40, and 45 weight percent, were prepared. The same mixing and centrifuging procedure used for type i) samples was followed. The three sets of samples (each in its plastic container) were then cured in ovens

at 50°C, 70°C, and 90°C. The 50°C and 70°C sample slugs were cured over night, the 90°C slug for 1.5 hours.

Preparation of samples for DSC. Samples for calorimetry were prepared by slicing and trimming a small quantity of each PDLC to fit into an aluminum DSC pan which was then hermetically sealed.[9,10] Sample weights ranged from about 8 mg to 17 mg.

Calorimetric Techniques

The differential scanning calorimeter used in these studies was a Perkin-Elmer DSC2 described previously.[1,2,9–12] The instrument was operated in its temperature scanning mode[9] in which the sample temperature was programmed linearly over the range of interest while changes in the sample's heat absorption rate, dQ/dt, were recorded. Sample temperatures as low as 190 K (−83°C) were attained by use of a Perkin-Elmer Intracooler II[10] refrigeration system. Glass transitions and first order phase transitions were analyzed using the instrument's thermal analysis data station and associated computer programs.[9–12]

Program (scanning) rates of 10 K/min and 20 K/min were used. [The slower rate was preferred for type i) samples based on 5CB and 7CB for which the nematic-isotropic transition temperatures were only slightly higher than the glass transition temperature of the matrix. The slower scan made it possible to resolve the glass and nematic-isotropic transitions fairly well (see below).] Plots of the heat absorption rate as a function of sample temperature then allowed us to determine phase transition temperatures and their associated transition enthalpies or specific heat changes. We shall illustrate the techniques by examining three DSC thermal spectra: one for a cured Bostik epoxy containing no LC, one for the pure 5CB LC, and one for a type i) PDLC formed by curing a mixture of the epoxy precursors with 5CB.

In Figure 1 is a DSC temperature scan for a sample of Bostik epoxy cured at 40°C. Only one feature is observed, a baseline shift associated with the glass transition of the polymer matrix material. The transition temperature, T_g(Matrix) [in this case 295 K (22°C)], is taken to be the temperature at which dQ/dt is half-way between baselines extrapolated from well below and well above the transition

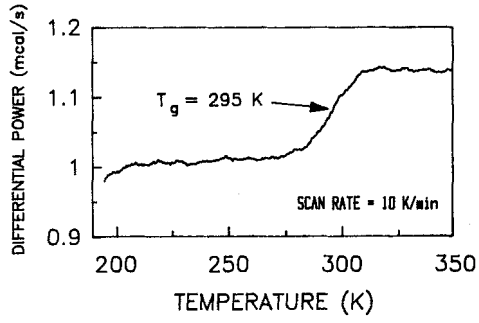

FIGURE 1 Differential scanning calorimetry (DSC) thermal scan for a Bostik epoxy cured at 40°C. A single glass transition is observed.

region. The magnitude of the increase in specific heat is $\Delta C_{\text{Matrix}} = 0.114$ cal/(g-K), as measured between the baselines. By convention, endothermic transitions in the DSC scans are plotted as upward-going.

Figure 2 shows a scan for the pure, single-component liquid crystal, 5CB. Several transitions are visible. Starting at low temperatures they are: i) a glass transition at T_g(LC) = 209 K (−64°C) with an associated specific heat increment $\Delta C_{\text{LC}} = 0.095$ cal/(g-K); ii) a crystallization exothermic peak at about 254 K (−19°C); iii) a melting endothermic peak at about 284 K (11°C); a small unidentified endotherm at about 290 K (17°C); and iv) a nematic-isotropic transition endotherm at $T_{\text{NI}} = 309$ K (36°C) with an associated transition enthalpy $\Delta H_{\text{NI}} = 0.85$ cal/g. The nematic-isotropic transition enthalpy was obtained from the peak area as measured between points of departure from the baselines above and below the transition. A few additional remarks may be helpful. It was possible to obtain the low temperature glassy state of 5CB merely by rapidly cooling the sample to 190 K at the ballistic cooling rate of the DSC. [As will be seen below, it was necessary to use a liquid nitrogen quench to obtain the glassy state of 7CB.] At the 254 K exotherm of Figure 2, the LC transformed from the metastable glassy state to a crystalline phase. The small peak at about 290 K was observed on only two of three scans, suggesting that it may be due to a metastable crystalline or smectic phase.

In Figure 3 is given a DSC scan for a 5CB/Bostik sample containing 33 weight percent liquid crystal. Only three transitions are observed: i) a LC glass transition at about 204 K (−69°C) with an associated $\Delta C_{\text{LC}} = 0.019$ cal/(g-K); ii) a matrix

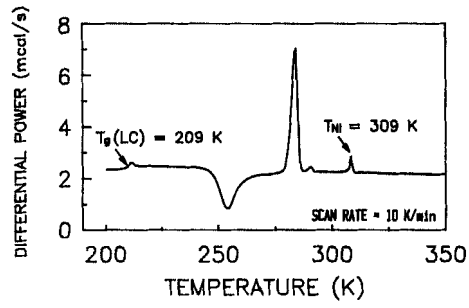

FIGURE 2 DSC scan for pure 5CB liquid crystal. The five transitions are discussed in the text.

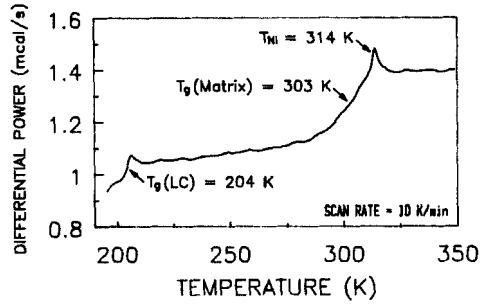

FIGURE 3 DSC scan for a 5CB/Bostik PDLC cured at 40°C. Liquid crystal concentration is 33 weight percent.

glass transition at T_g(Matrix) = 303 K (30°C) with ΔC_{Matrix} = 0.098 cal/(g-K); and a nematic-isotropic transition peak at 314 K (41°C) with ΔH_{NI} = 0.105 cal/g. Both the NI transition peak and the low temperature glass transition are due solely to liquid crystal contained within the microdroplets; the magnitudes of ΔH_{NI} and ΔC_{LC} thus measure the amount of LC in the droplets. Of considerable interest in Figure 3 is the absence of both the crystallization exotherm and the melting endotherm. It appears that confinement of the LC in the microdroplets tends to inhibit its crystallization for all samples of this system. The use of a scan rate of 10 K/min made it possible to resolve fairly well the matrix glass transition and the nematic-isotropic transition. [We hoped that even better resolution would be obtained for PDLC systems based on 7CB, with its slightly higher T_{NI}. However, as will be seen, only slight improvement in resolution was obtained.]

A series of DSC scans (at least two for each sample) like that of Figure 3 allowed us to determine values of T_g(LC), ΔC_{LC}, T_g(Matrix), ΔC_{Matrix}, T_{NI}, and ΔH_{NI} for the various PDLC samples of types i) and ii). Results will be presented below, along with analyses of the data which yield information regarding the fraction of LC in the droplets and the droplet number density (for 5CB-based systems).

Electron Microscopy

Droplet diameters for 5CB/Bostik PDLC samples (prepared using a procedure which we copied) had been measured by Golemme *et al.*[6] by means of electron microscopy (scanning and transmission). In our analysis we made use of their results (Figure 4).

EXPERIMENTAL RESULTS AND ANALYSIS

5CB/Bostik System

Phase diagram. Figure 5 shows a phase diagram for the 5CB/Bostik system. Transition temperatures are plotted as a function of X, the liquid crystal concentration in the PDLC (weight percent). All aspects of the figure are surprising: 1) The LC glass transition temperature increases slightly with LC content. We would

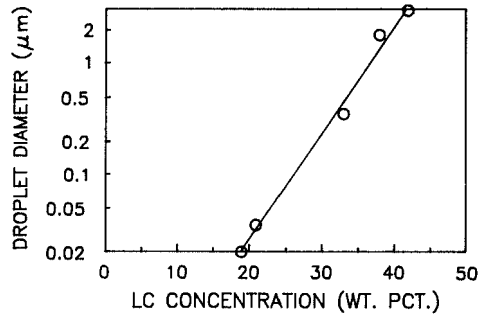

FIGURE 4 Microdroplet apparent diameter as a function of liquid crystal concentration for a 5CB/Bostik PDLC cured at 40°C. (From data of Reference 6).

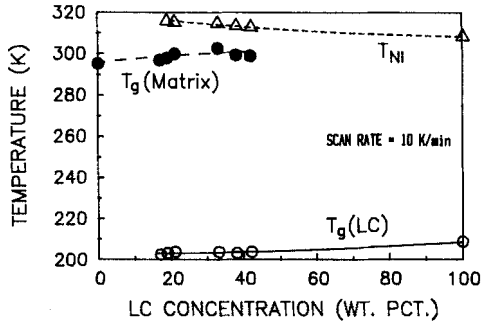

FIGURE 5 Phase diagram for a system of 5CB/Bostik PDLCs cured at 40°C.

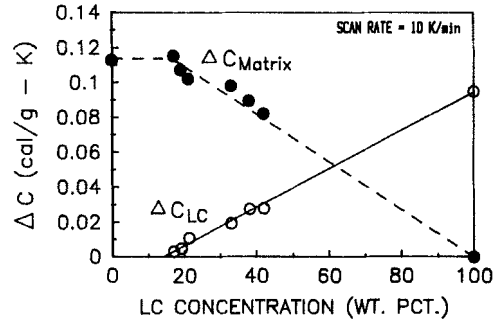

FIGURE 6 Specific heat increments at the glass transitions for liquid crystal in the microdroplets and for the polymer matrix of several 5CB/Bostik PDLCs cured at 40°C.

have expected T_g(LC) to decrease with a decrease in concentration of matrix oligomer molecules dissolved as impurities in the LC. 2) The matrix glass transition temperature appears to increase with LC content. Usually liquid crystal acts as a plasticizer, thereby decreasing T_g(Matrix). (There may actually be a slight downward trend for concentrations above 30%.) 3) The decrease in T_{NI} with LC concentration is contrary to expectations. We anticipated that, for low LC content, T_{NI} would be depressed due to dissolved impurity matrix molecules and that the magnitude of this depression would decrease as liquid crystal concentration increased. Indeed, the behavior of T_g(Matrix) and T_{NI} for the 5CB/Bostik system are contrary to that reported for a polyurethane-based PDLC containing a multicomponent liquid crystal.[11] [It should be kept in mind that possible interference between the matrix glass transition and the nematic-isotropic transition may, in part, account for discrepancies 2) and 3).]

ΔC_{LC} and ΔH_{NI}. Of greater interest than the transition temperatures are the specific heat increments at the glass transitions and the nematic-isotropic transition enthalpy. Figure 6 plots both ΔC_{LC} and ΔC_{Matrix} as a function of the liquid crystal concentration. The matrix increment, ΔC_{Matrix}, remains roughly constant for low values of X and then decreases linearly to zero at $X = 100\%$. In contrast, ΔC_{LC} increases linearly with X above an intercept $A = 14\%$. This intercept is the solubility limit of liquid crystal in the matrix. Figure 7 shows the dependence of ΔH_{NI} on

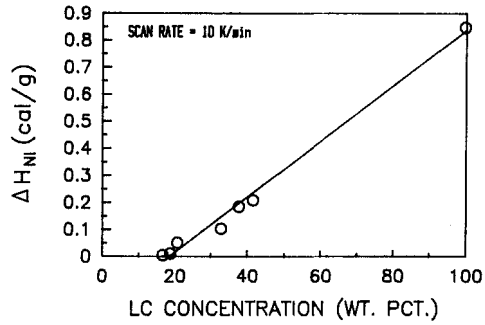

FIGURE 7 Nematic-isotropic transition enthalpy for liquid crystal in the microdroplets of several 5CB/Bostik PDLCs cured at 40°C.

LC concentration. As for ΔC_{LC}, a linear dependence is seen, but with a somewhat higher X-axis intercept (about 19%).

Smith[11] has derived an expression for the dependence of the nematic-isotropic transition enthalpy on LC concentration:

$$P = (X - A)/(100 - A) \qquad (X \geq A), \tag{1}$$

where $P = \Delta H_{NI}(X)/\Delta H_{NI}(LC)$, the ratio of the nematic-isotropic transition enthalpy for a sample containing X weight percent LC to that for the pure liquid crystal. He also showed that experimental data for a polyurethane-based PDLC are fairly well described by equation (1). Although originally derived for the nematic-isotropic transition enthalpy, equation (1) is equally valid for the LC specific heat increment. [The corresponding expression for the specific heat increment uses $P = \Delta C_{LC}(X)/\Delta C_{LC}(LC)$.] The derivation was based on two assumptions:

1) Only LC which is not dissolved in the matrix contributes to ΔH_{NI} and to ΔC_{LC}. For low enough liquid crystal concentrations (depending on the PDLC, the limiting X could be on the order of or less than 45%) this undissolved LC is essentially all contained within the microdroplets.

2) The amount of LC which a given mass of matrix can dissolve is the same everywhere along the curve of P versus X for $X \geq A$.

Within the limits of these assumptions, equation (1) is exact if X is expressed as a weight percent. For X as a volumetric percent, equation (1) is a good approximation, providing the polymer and LC densities are roughly equal.[11]

The fact that ΔC_{LC} and ΔH_{NI} (Figures 6 and 7) are well described by straight lines, is taken as strong support for the validity of equation (1) and its underlying assumptions. For low LC concentrations both ΔC_{LC} and ΔH_{NI} are proportional to the amount of liquid crystal in the microdroplets. For higher X values, where a "reversed" or "polymer ball morphology"[13] would be observed, equation (1) would still be valid. However, P would no longer be proportional to the amount of LC contained in the microdroplets; instead, it would be a measure of all liquid crystal not dissolved in the matrix (and would thus include "puddles" and "pools" of LC). It should be stressed that in Golemme's 5CB/Bostik PDLCs droplet morphologies were always observed, even for the largest LC concentrations.[6]

The linear regression fit for ΔC_{LC} (Figure 6) is slightly better than that for ΔH_{NI} (Figure 7); $r^2 = 0.996$ for the former, 0.992 for the latter. The standard error of estimate for ΔC_{LC} is 0.0023 cal/g-K; that for ΔH_{NI} is 0.029 cal/g. The lower value of A from ΔC_{LC} ($A = 14$) than from ΔH_{NI} ($A = 18.9$) is probably due to the intrinsic temperature dependence of the LC solubility in the matrix (see DISCUSSION).

Fraction of LC in Microdroplets. From ΔC_{LC} and ΔH_{NI} it is possible to estimate α, the fraction of liquid crystal contained within the microdroplets. However, this determination is subject to the restriction that the LC concentration must fall within the range for microdroplets rather than for "reversed morphology." The basic expression for the calculation of α from ΔH_{NI} (or ΔC_{LC}) was given by Smith and Vaz[9]:

$$\alpha = (1 + F)P, \tag{2}$$

where $F = m_p/m_{LC}$, the ratio of polymer liquid crystal mass in the sample. Equation (2) can be rewritten as

$$\alpha = (100/X)P. \tag{3}$$

Combining equations (1) and (3) gives

$$\alpha = 0 \qquad (X < A)$$

$$\alpha = (100/X)(X - A)/(100 - A) \qquad (X \geq A). \tag{4}$$

Of considerable importance is the fact that equation (4) predicts that the fraction of liquid crystal contained within the microdroplets is a function only of X and the solubility limit, A.

In Figure 8 are plotted α values derived from the LC specific heat increment and from the transition enthalpy. The points were calculated by substituting measured values of ΔC_{LC} and ΔH_{NI} into equation (3). The smooth curves are plots of

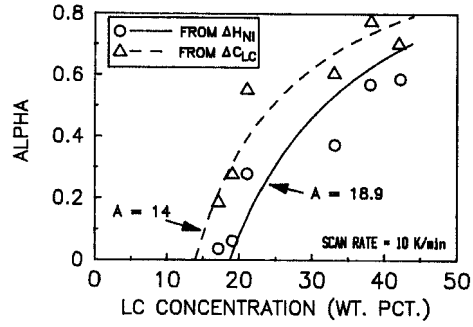

FIGURE 8 Fraction of liquid crystal contained in microdroplets for a 5CB/Bostik PDLC system cured at 40°C.

equation (4) using A-values derived from the linear fits to the data of Figures 6 and 7. The smooth curves are much more reliable estimates of the fraction of liquid crystal in the droplets than are the points. The reason for this is straightforward: As can be seen from Figures 6 and 7, the raw data for ΔC_{LC} and ΔH_{NI} are fit extremely well by equation (1), yielding reliable values of A from which α can be determined using equation (4). On the other hand, computation of α by substituting raw data directly into equation (3) has greater uncertainty since, for low LC concentrations, the experimental error (as estimated by the standard error) is comparable to the measured values of ΔC_{LC} or ΔH_{NI}.

Estimate of droplet number density. Smith,[11] from an analysis of calorimetric data and an examination of SEM micrographs for two different PDLC systems, found the following relation for volumetric droplet number density:

$$n_V = \text{const} \times D^{-z}, \tag{5}$$

where $z = 1.9$ to 2 for a polyurethane-based PDLC and $z = 2.48$ to 2.75 for an epoxy-based system. From the droplet size data of Reference 6 and our ΔC_{LC} and ΔH_{NI} results, we can calculate corresponding expressions for the 5CB/Bostik system. To do this, we need to know the functional relationships (if any) of ΔC_{LC} and ΔH_{NI} to D. [That such relationships exist is reasonable, since the calorimetric quantities are proportional to the mass of LC in the droplets. Even if there are no functional relations between the DSC quantities and D, the equation we shall derive will allow us to compute n_V from ΔC_{LC} and ΔH_{NI}.]

In Figures 9 and 10 are given logarithmic plots of ΔC_{LC} and ΔH_{NI} versus the droplet size data of Reference 6. The solid lines are linear fits to all five data points; the dashed lines are fits which exclude the data point for the smallest droplet ($D = 0.02$ μm). It is valid to exclude this point for which the magnitudes of ΔC_{LC} and ΔH_{NI} are so small that they are comparable to the experimental errors. The dashed lines are much better fits to the four data points ($r^2 = 0.988$ for Figure 9; $r^2 = 0.999$ for Figure 10) than are the solid lines to the five points ($r^2 = 0.893$ and 0.845 for Figures 9 and 10 respectively). We shall restrict our attention to the four-point fits.

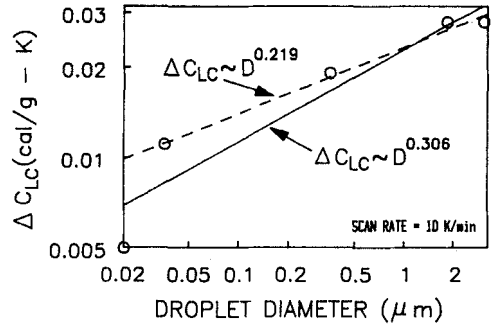

FIGURE 9 Liquid crystal specific heat increment as a function of droplet diameter for a 5CB/Bostik PDLC system cured at 40°C. Droplet diameters are from Reference 6.

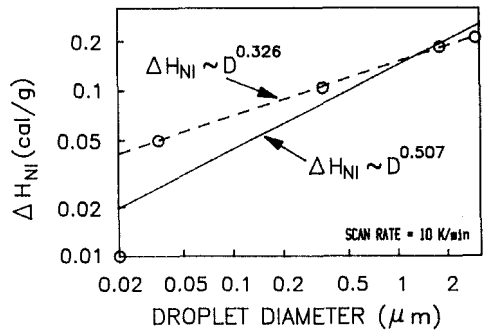

FIGURE 10 Nematic-isotropic transition enthalpy as a function of droplet diameter for a 5CB/Bostik PDLC system cured at 40°C. Droplet diameters are from Reference 6.

The data of Figure 9 (dashed line) are well expressed by

$$\Delta C_{LC} = 0.0234 \times D_a^{0.219} \qquad (D_a \text{ in } \mu\text{m}), \tag{6}$$

and the data of Figure 10 (dashed line) by

$$\Delta H_{NI} = 0.149 \times D_a^{0.326} \qquad (D_a \text{ in } \mu\text{m}), \tag{7}$$

where D_a is the "apparent" droplet diameter as measured by electron microscopy. As pointed out elsewhere,[11,14] the apparent diameter is related to the "true" droplet diameter, D_t, by $D_a = \pi D_t/4$.

It is a simple matter to use equations (2) and (6) [or (2) and (7)] to derive an expression for n_V. Equation (2) can be rearranged to give

$$\Delta C_{LC}(X) = \frac{m_{LC}^D}{m_{tot}} \Delta C_{LC}(LC). \tag{8}$$

where m_{LC}^D is the mass of LC in the droplets and m_{tot} is the total PDLC mass. The mass of LC in the droplets is

$$m_{LC}^D = \rho_{LC} \times V_D \times N_D = \rho_{LC} \times \frac{\pi D_t^3}{6} N_D, \tag{9}$$

where V_D is the volume of a droplet, N_D is the total number of droplets, D_t is the true droplet diameter, and ρ_{LC} is the liquid crystal density. The total PDLC mass is

$$m_{tot} = \rho_{PDLC} \times V_{tot}, \tag{10}$$

where ρ_{PDLC} is the PDLC density and V_{tot} is the total PDLC volume. Substituting equations (9) and (10) into equation (8) gives

$$\Delta C_{LC}(X) = \frac{\pi \rho_{LC}}{6\rho_{PDLC}} \frac{N_D D_t^3}{V_{tot}} \Delta C_{LC}(LC) \simeq \frac{\pi}{6} n_V D_t^3 \Delta C_{LC}(LC). \tag{11}$$

Thus,

$$n_V \simeq \frac{6}{\pi D_t^3} \frac{\Delta C_{LC}(X)}{\Delta C_{LC}(LC)}. \tag{12}$$

Here we have used the fact that $n_V = N_D/V_{tot}$; also, the "$\simeq$" sign is due to the assumption that the densities of the LC and the PDLC are approximately equal. A similar expression for the nematic-isotropic enthalpy is obtained by replacing ΔC_{LC} by ΔH_{NI} in numerator and denominator.

Substituting equation (12) into equation (6), rearranging and using the relation between D_t and D_a, gives the desired expression for n_V:

$$n_V = 0.23 \times D_a^{-2.78}\ \mu m^{-3} \qquad (\text{from } \Delta C_{LC},\ D_a \text{ in } \mu m) \tag{13}$$

$$= 1.74 \times D_a^{-2.78}\ cm^{-3} \qquad (D_a \text{ in cm}). \tag{13a}$$

The corresponding equation derived from ΔH_{NI} is

$$n_V = 0.31 \times D_a^{-2.67}\ \mu m^{-3} \qquad (\text{from } \Delta H_{NI},\ D_a \text{ in } \mu m) \tag{14}$$

$$= 3.27 \times D_a^{-2.67}\ cm^{-3} \qquad (D_a \text{ in cm}), \tag{14a}$$

We have written the equations in terms of D_a since that is the droplet diameter as measured from SEMs. It is noteworthy that the two sets of equations are quite similar in the magnitudes of their coefficients and exponents, in spite of the differences in equations (6) and (7). The previous calorimetric/SEM study of an E7/epoxy PDLC system[11] yielded the following relation:

$$n_V = 2.68 \times D_a^{-2.75}\ cm^{-3} \qquad (D_a \text{ in cm}). \tag{15}$$

It should be emphasized that the procedures for varying droplet size and number density in Reference 11 were quite different from those of the present work. In the previous study, LC concentration was held constant while cure rate was varied by adjusting the cure temperature. In the present case, cure temperature was held constant while LC concentration was varied. The fact that, in spite of these differences in sample preparation and composition, there is good agreement between equation (15) and equations (13a) and (14a) suggests that the relationship between number density and droplet size may be rather general. Smith[11] also determined a relation between n_V and D for the E7/epoxy PDLC system from a droplet count of SEM micrographs, obtaining a slightly lower exponent ($z \simeq -2.5$). Considering the experimental uncertainties in both DSC and micrography, we feel that the results from the various analyses are fairly consistent.

7CB/Bostik System

As mentioned above, pure 7CB and its PDLC systems exhibit phase behavior which differs to some extent from that of 5CB and its PDLCs. The glassy state of pure 7CB could only be attained by quenching the liquid crystal (encapsulated in

its aluminum sample pan) to liquid nitrogen temperature and then immediately placing it in the calorimeter at 190 K, using cold tweezers. The DSC thermal spectrum was then obtained by scanning the temperature at 10 K/min. Figure 11 shows a resulting spectrum. Six transitions are apparent: the LC glass transition at T_g(LC) = 209 K (−64°C) with ΔC_{LC} = 0.088 cal/g-K; three successive exotherms at about 225 K (−48°C), 240 K (−33 K), and 270 K (−3°C); a melting endotherm at about 306 K (33°C); and the nematic-isotropic transition at T_{NI} = 315 K (44°C), with ΔH_{NI} = 1.16 cal/g.

The glassy state of all our 7CB/Bostik PDLC samples was attainable merely by cooling to 190 K at the DSC instrument's fastest ballistic rate. For PDLCs with LC concentrations greater than 33 weight percent, it was possible to crystallize (at least to some extent) the liquid crystal in the microdroplets. Evidence for this behavior is seen in Figures 12 and 13. The DSC spectrum for a sample with X = 42% (Figure 12) exhibits two low temperature exotherms, the lowest of which involves a transformation from the glassy state. Two large endotherms (at about 295 K and 307 K) are probably due to crystal-crystal and crystal-nematic transitions. The small high temperature endotherm is due to the nematic-isotropic transition. Figure 13 (for X = 38%) shows the LC glass transition, one or two weak exotherms, the 295 K endotherm (considerably reduced from that of Figure 12), and the NI peak. The fact that LC could be crystallized in samples of 7CB/epoxy PDLCs

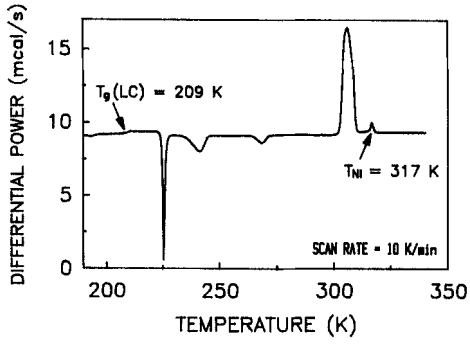

FIGURE 11 DSC scan for pure 7CB. Phase transitions are discussed in the text.

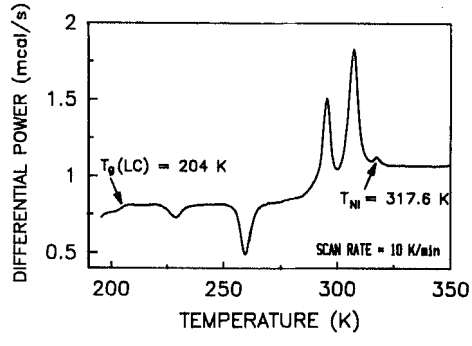

FIGURE 12 DSC scan for 7CB/Bostik PDLC cured at 40°C. The liquid crystal concentration was 42 weight percent.

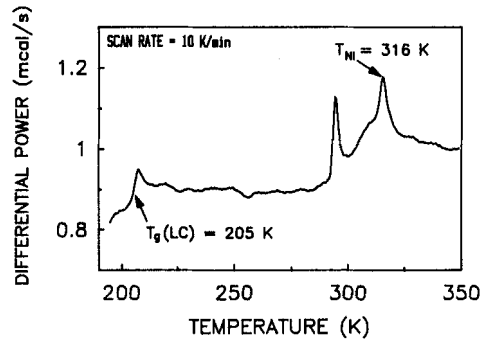

FIGURE 13 DSC scan for 7CB/Bostik PDLC cured at 40°C. The liquid crystal concentration was 38 weight percent.

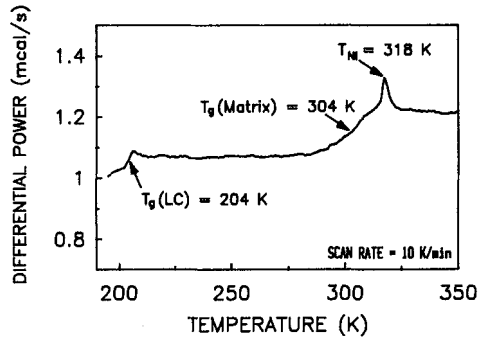

FIGURE 14 DSC scan for 7CB/Bostik PDLC cured at 40°C. The liquid crystal concentration was 33 weight percent.

having large X-values is in marked contrast with the behavior for 5CB/epoxy samples, for which the LC did not crystallize.

It is clear from Figures 12 and 13 that the large endotherms make it difficult to determine the temperature and specific heat increment of the matrix glass transition; furthermore, the 307 K endotherm partially obscures the nematic-isotropic transition. In order to fully reveal both the matrix glass transition and the nematic-isotropic transition of these two samples, it was necessary to suppress crystallization in the samples with $X = 38\%$ and 42%. This was accomplished by cooling from room temperature to about 260 K [below T_g(Matrix) but above the crystallization temperature] and subsequently carrying out a DSC scan.

No indication of a crystalline phase is seen in the DSC spectrum for $X = 33\%$ (Figure 14). In fact, crystallization is not detected for any sample with $X < 33\%$. Evidentially crystallization is suppressed in sufficiently small droplets. The possibility of an induced smectic phase must not be ruled out for intermediate concentrations ($X > 35\%$).

Phase diagram. The phase diagram of the 7CB/Bostik system (Figure 15) shows some of the same unexpected behavior as the 5CB-based PDLC (Figure 5). Both glass transition temperatures appear to increase with increasing LC concentration.

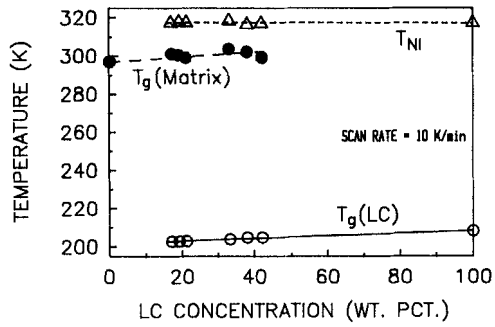

FIGURE 15 Phase diagram for 7CB/Bostik PDLC system cured at 40°C.

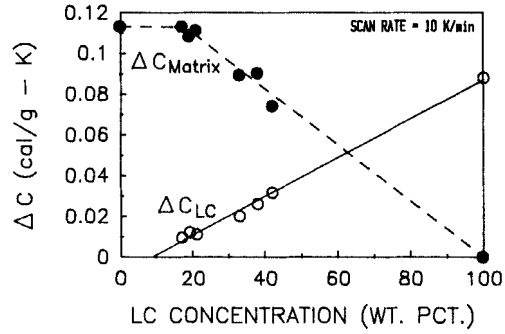

FIGURE 16 Specific heat increments at the glass transitions for liquid crystal in the microdroplets and for the polymer matrix of several 7CB/Bostik PDLCs cured at 40°C.

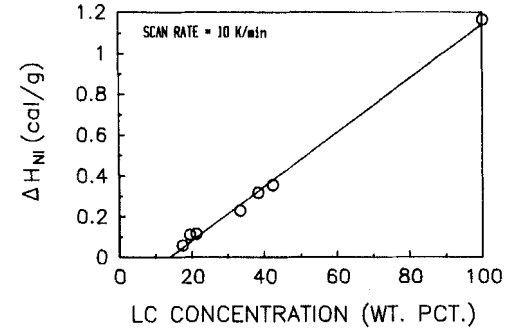

FIGURE 17 Nematic-isotropic transition enthalpy for liquid crystal in the microdroplets of several 7CB/Bostik PDLCs cured at 40°C.

[Once again T_g(Matrix) appears to decrease slightly above $X = 30\%$.] T_{NI} remains essentially constant over the entire range of concentration.

ΔC_{LC} and ΔH_{NI}. The concentration dependences of the specific heat increments and the nematic-isotropic transition enthalpy (Figures 16 and 17) are similar to those for the 5CB-based system. Linear regression analyses of ΔC_{LC} and ΔH_{NI} yield excellent fits; $r^2 = 0.995$ for the former, 0.996 for the latter. The standard

error of estimate for ΔC_{LC} is 0.0021 cal/g-K; that for ΔH_{NI} is 0.025 cal/g. Both errors are comparable to those for the 5CB/Bostik system. As for the 5CB PDLCs, ΔC_{LC} gives a lower value of A (A = 9) than does ΔH_{NI} (A = 13.6), probably due to the temperature-dependent solubility. The fact that the A-values for the 7CB/epoxy system are somewhat lower than the corresponding ones for the 5CB PDLCs suggests that 7CB is slightly less soluble in the matrix than is 5CB. This result may be ascribable to the higher molecular weight of 7CB.

Fraction of LC in microdroplets. In Figure 18 are plotted the dependences of α on LC concentration as determined from ΔC_{LC} and ΔH_{NI}. Once again the points represent values calculated directly from equation (3) using measurements of ΔC_{LC} and ΔH_{NI}. The smooth curves, determined from equation (4) are, of course, more reliable. As for the 5CB systems, the agreement of the two curves is felt to be acceptable, considering experimental uncertainties.

E7/Epoxy System

As mentioned above, the liquid crystal used in this system was E7, a four component mixture. Since E7 was slow to crystallize upon cooling, its DSC spectrum (taken at a scan rate of 20 K/min) exhibited only a low temperature glass transition [T_g (LC) = 213 K (−60°C), ΔC_{LC} = 0.095 cal/g-K] and a nematic-isotropic transition [T_{NI} = 334 K (61°C)]. In the present study we re-measured ΔH_{NI}(LC) to be 1.09 cal/g, somewhat higher than reported previously (0.91 cal/g).[9]

The glass transition temperature of the index-matched epoxy (T_g(Matrix) ≃ 260 K (−13°C)] is considerably lower than that of the Bostik epoxy. Furthermore, the corresponding specific heat increment [ΔC(Matrix) ≃ 0.16 cal/g-K] is somewhat larger than that of Bostik. Both of these facts suggest that the Bostik is more fully cross-linked than the index-matched epoxy.

As seen in Figure 19, the DSC spectra of the E7/epoxy PDLC systems exhibit only three transitions: a low temperature glass transition due to LC in the microdroplets, a matrix glass transition, and a nematic-isotropic transition peak. The details of these phase transitions will be reported in the next sections.

Phase diagram. Figure 20 shows the dependence of the E7/epoxy transition

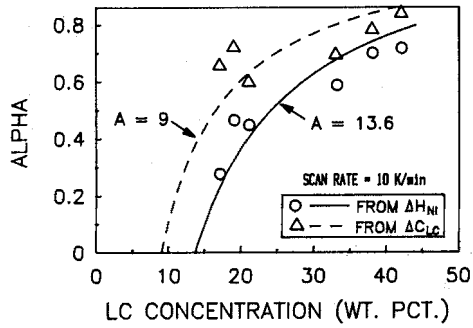

FIGURE 18 Fraction of liquid crystal contained in microdroplets for a 7CB/Bostik PDLC system cured at 40°C.

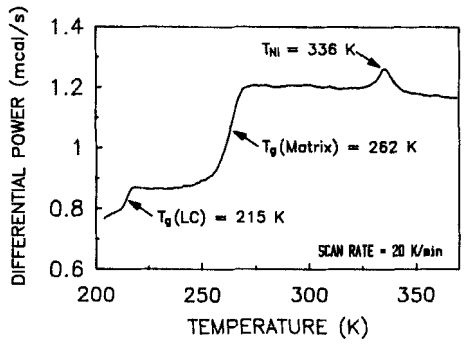

FIGURE 19 DSC scan for a PDLC containing 25 weight percent E7 in an index-matched epoxy matrix. Cure temperature was 70°C.

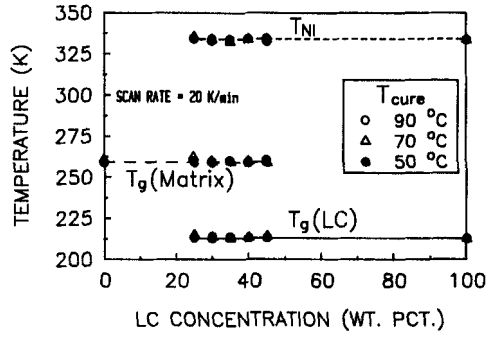

FIGURE 20 Phase diagrams for E7/epoxy PDLC systems cured at three different temperatures.

temperatures on liquid crystal concentration and cure temperature. It is clear that T_g(LC), T_g(Matrix), and T_{NI} are all relatively insensitive to both of these variables. The behavior of T_g(Matrix) and T_{NI} is dissimilar to that for a polyurethane-based PDLC system[11] for which the matrix glass transition temperature decreases appreciably with X, while the nematic-isotropic transition temperature increases.

ΔC_{LC} and ΔH_{NI}. The dependences of the specific heat increment on LC concentration are shown in Figure 21. Although the scatter in ΔC_{Matrix} is sizable, the matrix specific heat increment exhibits the same general trend as for the Bostik-based samples. It appears that ΔC_{LC} is rather insensitive to cure temperature, with one exception: for X = 45% and T_{cure} = 50°C, the LC specific heat increment is too low. Therefore, this point was excluded in carrying out the regression which yielded the linear fit of Figure 21. The best fits for the three cure temperatures all gave similar values of the solubility limit, A, which ranged from 12 to 15.

Figure 22 plots the concentration-dependence of the nematic-isotropic transition enthalpy for the E7/epoxy systems. In this case, the data for T_{cure} = 90°C yield the highest value of A. Once again the data point for X = 45% and T_{cure} is much too low and was ignored in the linear regression. The low values of both ΔC_{LC} and ΔH_{NI} for this sample (prepared with the highest LC concentration and at the lowest cure temperature) suggest that a large fraction of the liquid crystal is dissolved in the matrix. This may possibly be due to a low degree of cure for this sample.

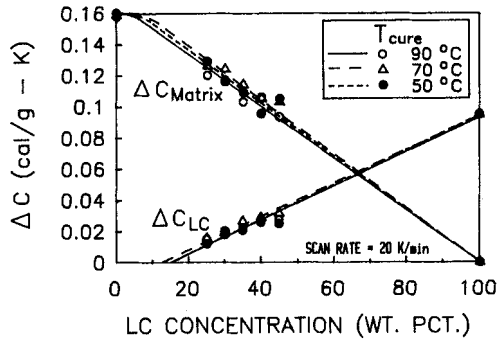

FIGURE 21 LC and matrix specific heat increments for E7/epoxy PDLCs cured at three different temperatures.

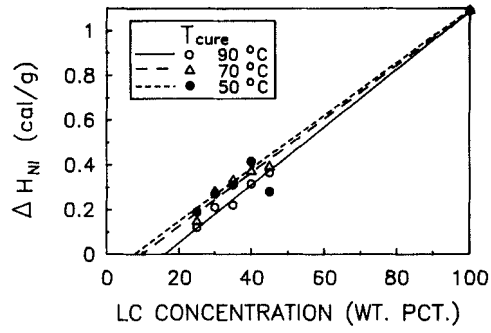

FIGURE 22 Nematic-isotropic transition enthalpies for LC in the microdroplets of E7/epoxy PDLCs cured at three different temperatures.

The A-values from ΔC_{LC} and ΔH_{NI} are comparable in magnitude for the samples cured at 70°C and 90°C. For the one cured at 50°C the A-value from ΔC_{LC} is appreciably smaller than that from ΔH_{NI}. This discrepancy may be due, in part, to incomplete cure at the lower temperature. Furthermore, the fact that the liquid crystal (E7) is a four-component system may result in preferential solution of some of its components in the matrix, which would complicate the determination of A from the DSC measurements.

Fraction of LC in microdroplets. As for both Bostik-based samples, the best estimates of α are calculated from equation (4) using A-values obtained from the linear fits to the data for ΔC_{LC} and ΔH_{NI}. The results are shown as smooth curves in Figures 23–25. Also shown, as points, are values determined from equation (3) and the raw DSC data. The agreement of α-values for the two highest cure temperatures is reasonably good. The disagreement for samples cured at 50°C may be due to a cure which was possibly incomplete.

DISCUSSION

Calorimetric studies are extremely valuable in helping us to assess and optimize PDLC properties. From the linear dependence of both ΔC_{LC} and ΔH_{NI} on LC

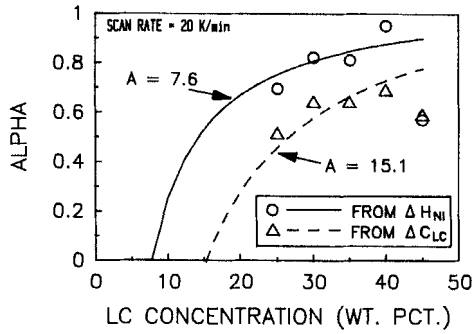

FIGURE 23 Fraction of liquid crystal contained in microdroplets for an E7/epoxy PDLC system cured at 50°C.

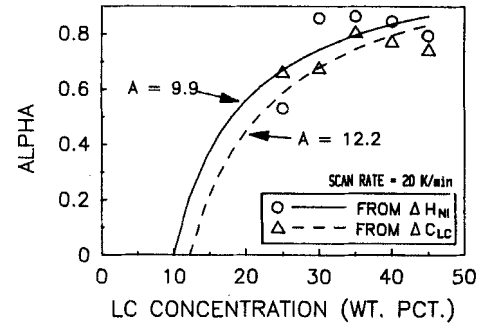

FIGURE 24 Fraction of liquid crystal contained in microdroplets for an E7/epoxy PDLC system cured at 70°C.

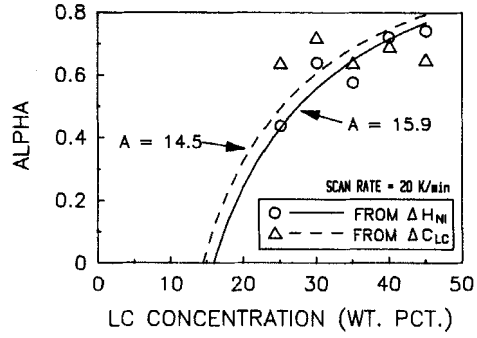

FIGURE 25 Fraction of liquid crystal contained in microdroplets for an E7/epoxy PDLC system cured at 90°C.

concentration [equation (1)] we can obtain A, the solubility limit of the liquid crystal in the matrix.[15] This one parameter then allows us to compute α, the fraction of LC in the microdroplets. When coupled with electron microscopy measurements of droplet sizes, the DSC results also allow us to calculate droplet number densities.

The ideal PDLC would be one in which all the liquid crystal is contained in the

microdroplets and none in the matrix. Such a system is, of course, unattainable, but calorimetric studies of various LC/matrix candidates would allow us to choose a combination for which phase separation is most complete. Equation (4) can provide some guidance in the choice. We rewrite the equation in the form

$$\alpha \times [(100 - A/100)] = 1 - A/X, \tag{16}$$

and plot it in Figure 26. This expression is a function only of A and X, the liquid crystal concentration. It is apparent that a low value of A is needed in order to maximize phase separation. For example, if $A < 5$, an α value on the order of 0.95 can be achieved for $X \simeq 50\%$. For $A = 3$, the same degree of separation could be attained with $X \simeq 36\%$. Obviously, for $A = 0$, α would always equal 1. For our thermally-cured epoxy-based PDLCs, the lowest A value attained was about 8 weight percent. The selection of liquid crystal/polymer matrix combinations with lower A values could, perhaps, be assisted by solubility theory[16,17]; DSC measurements of ΔC_{LC} and ΔH_{NI} could then provide an empirical check on the predictions of the theory.

At a recent symposium on PDLCs[18] there was some discussion of the discrepancy between the A-values derived from ΔC_{LC} and ΔH_{NI}. It was suggested that this difference is due to the temperatures at which the quantities were determined. Since ΔC_{LC} was measured near 200 K and ΔH_{NI} about 100 K higher, a lower LC solubility in the matrix would be expected at the lower temperature, in agreement with the A-values found for the 5CB and 7CB PDLCs. It should be pointed out that the PDLC phase diagram calculated by Hirai *et al.*[19] can be interpreted to predict an A-value which increases with temperature.

The present study confirms that droplet number density has a simple dependence on droplet diameter [equation (5)]. For thermally-cured epoxy-based PDLCs, this expression seems to be fairly insensitive to methods of sample preparation; similar results were obtained for samples in which n_V and D were varied by quite different techniques. For good PDLC light scattering properties n_V should be as large as possible. Equation (5) indicates that a large number density can be achieved by decreasing droplet diameter; however, previous work[3] has shown that there is an optimum droplet diameter for best electro-optic performance. Thus, a compromise may have to be made in the choices of n_V and D.

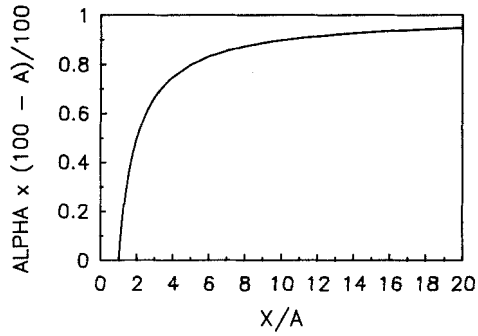

FIGURE 26 Theoretical dependence of $\alpha \times (100 - A)/100$ on X/A.

In this paper we have not focussed on ΔC_{Matrix}, the specific heat increment at the matrix glass transition, although from Figures 6, 16, and 21, it is apparent that is is also sensitive to LC concentration. There may be additional information to extract from this parameter, particularly for non-mesogenic systems (see below). For PDLCs, we feel that ΔC_{LC} and ΔH_{NI} are more useful.

It should be pointed out that our methods may be of value in studying phase separation in microdispersions of non-mesogenic systems. Such studies would not, of course, involve determinations of ΔH_{NI}. However, if the dispersed liquid has an accessible glass transition, it would be possible to measure the concentration-dependence of the associated specific heat increment and use it to compute A and α values for the system. Furthermore, the concentration dependence of ΔC_{Matrix} could provide useful information.

Acknowledgments

The authors thank T. H. VanSteenkiste, D. B. Hayden, and W. D. Marion for valuable technical assistance and N. A. Vaz, G. P. Montgomery, Jr., and J. W. Doane for useful discussions.

References

1. N. A. Vaz, G. W. Smith and G. P. Montgomery, Jr., *Mol. Cryst. Liq. Cryst.*, **146**, 17 (1987).
2. N. A. Vaz, G. W. Smith and G. P. Montgomery, Jr., *Mol. Cryst. Liq. Cryst.*, **146**, 1 (1987).
3. G. P. Montgomery, Jr., J. L. West and W. Tamura-Lis, *J. Appl. Phys.*, **69**, 1605 (1991).
4. Bostik Division of Emhart Corp., Middleton, MA.
5. Manufactured by BDH, Ltd. Distribution by EM Industries, Inc., Hawthorne, NY.
6. A. Golemme, S. Zumer, D. W. Allender and J. W. Doane, *Phys. Rev. Lett.*, **61**, 2937 (1988).
7. Manufactured by Shell Chemical Co., Distributed by Miller-Stephenson Chemical Co., Morton Grove, IL.
8. Wilmington Chemical Corp., Wilmington, DE.
9. G. W. Smith and N. A. Vaz, *Liq. Cryst.*, **3**, 543 (1988).
10. Perkin-Elmer Corp., Norwalk, CT.
11. G. W. Smith, *Mol. Cryst. Liq. Cryst.*, **180B**, 201 (1990).
12. G. W. Smith, *Mol. Cryst. Liq. Cryst.*, **196**, 89 (1991).
13. F. G. Yamagishi, L. J. Miller and C. I. van Ast, *Proc. SPIE*, **1080**, 53 (1989).
14. G. P. Montgomery, Jr., private communication.
15. N. A. Vaz (private communication) has pointed out that A-values can also be estimated from observations of the concentration dependence of PDLC refractive index and light scattering, as well as from SEM studies of morphology.
16. A. F. M. Barton, *Handbook of Solubility Parameters and Other Cohesion Parameters*, CRC Press, Boca Raton, FL, 1983.
17. A. F. M. Barton, *Handbook of Polymer-Liquid Interaction Parameters and Solubility Parameters*, CRC Press, Boca Raton, FL, 1990.
18. First ALCOM Symposium on Dispersions of Liquid Crystals and Polymers, Cuyahoga Falls, OH, June 12–13, 1991.
19. Y. Hirai, S. Niiyama, H. Kubai and T. Gunjima, *SPIE*, **1257**, 2 (1990).